ORIGINAL ARTICLE

การอ้างอิงอยู่ในหน้า 8

A C G publications

Rec. Nat. Prod. 18:3 (2024) 331-338

records of natural products

Antimicrobial and *α*-Glucosidase Inhibitory Compounds from the Branches of *Uvaria siamensis*

Ngoc-Hong Nguyen [1], Boi-Phong Vuong [2], Chuong Hoang Nguyen [3], A. Dong Huynh [3], Dinh-Manh Nguyen [2], Thuc-Huy Duong [2], Hoang-Thanh Kpa [2], Thi-Kim-Dung Le [4,5], Thi-Ngoc-Duyen Nguyen [2], Huy Truong Nguyen [4*] and Jirapast Sichaem [6*]

[1]*CirTech Institute, HUTECH University, 475 A Dien Bien Phu Street, Binh Thanh District, Ho Chi Minh City, Vietnam*
[2]*Department of Chemistry, Ho Chi Minh City University of Education, 280 An Duong Vuong Street, District 5, Ho Chi Minh City 748342, Vietnam*
[3]*Faculty of Biology and Biotechnology, University of Science, Vietnam National University Ho Chi Minh City, Ho Chi Minh City 700000, Vietnam*
[4]*Faculty of Pharmacy, Ton Duc Thang University, Ho Chi Minh City 700000, Vietnam*
[5]*Laboratory of Biophysics, Institute for Advanced Study in Technology, Ton Duc Thang University, Ho Chi Minh City 700000, Vietnam*
[6]*Research Unit in Natural Products Chemistry and Bioactivities, Faculty of Science and Technology, Thammasat University Lampang Campus, Lampang 52190, Thailand*

(Received February 20, 2024; Revised March 21, 2024; Accepted March 22, 2024)

Abstract: A new *γ*-butenoid, (*Z*)-6-acetylsphaerodol (**2**), along with seven known compounds, (4*E*)-7-benzoyloxy-6-hydroxy-2,4-heptadien-4-olide (**1**), (6*S*)-melodorinol (**3**), (6*S*)-acetylmelodorinol (**4**), (*Z*)-sphaerodiol (**5**), (*Z*)-7-acetylsphaerodol (**6**), dichamanetin (**7**), and pinocembrin (**8**), were isolated and structurally elucidated from *Uvaria siamensis* growing in Thailand. Their chemical structures were assigned by extensive spectroscopy (NMR and HRESIMS), as well as comparisons with the previous literature. Compounds **1-8** were evaluated for the antimicrobial activity against two multidrug-resistant *Staphylococcus aureus* strains, 23Sa1 and SA-ATCC. Compounds **4** and **6** displayed moderate activity with inhibitory zones of 13 and 12 mm against 23Sa1 and SA-ATCC strains, respectively. Compounds **3** and **7** exhibited significant efficacy, displaying IC_{50} values of 157.7 and 94.2 µM, respectively, against *α*-glucosidase. According to the docking data, compounds **3** and **7** have a greater influence on binding contacts with the *α*-glucosidase active pocket, thereby affecting the inhibitory activity of the enzyme.

Keywords: Annonaceae; *Uvaria siamensis*; (*Z*)-6-acetylsphaerodol; *γ*-butenoid; antimicrobial activity; *α*-glucosidase inhibition.

* Corresponding author: E-Mail: nguyentruonghuy@tdtu.edu.vn (H. T. Nguyen) jirapast@tu.ac.th (J. Sichaem)

The article was published by ACG Publications
http://www.acgpubs.org/journal/records-of-natural-products May-June 2024 EISSN:1307-6167
DOI: http://doi.org/10.25135/rnp.452.2402.3145
Available online: April 08, 2024

1. Introduction

Uvaria siamensis (Scheff.) L.L. Zhou, Y.C.F. Su, & R.M.K. Saunders, a member of the Annonaceae family, is commonly found in Asian countries such as Thailand and Vietnam [1-3]. In Thailand, this plant is known as "Lamduan", and its flower holds significance in Thai traditional medicine for its roles as a tonic, mild cardiotonic stimulant, hematinic, and antipyretic [4]. To date, more than 80 compounds have been identified in this species under the names *U. siamensis* and *M. fruticosum* (recognized as a synonym), including *γ*-butenolides, chalcones, flavanols, and alkaloids [2, 4-13]. The extracts and compounds obtained from *U. siamensis* exhibited diverse pharmaceutical properties, including cytotoxicity [14-16], antifungal and antioxidant activities [8, 17], anti-inflammatory effects [5, 18], antiplasmodial activity [19], and *α*-glucosidase inhibitory activity [14, 20, 21]. In this investigation, we present the isolation and structural interpretation of a novel *γ*-butenoid, (*Z*)-6-acetylsphaerodol (**2**), together with seven known compounds, (4*E*)-7-benzoyloxy-6-hydroxy-2,4-heptadien-4-olide (**1**) [13], (6*S*)-melodorinol (**3**) [13], (6*S*)-acetylmelodorinol (**4**) [13], (*Z*)-sphaerodiol (**5**) [22], (*Z*)-7-acetylsphaerodol (**6**) [22], dichamanetin (**7**) [22], and pinocembrin (**8**) [22] (Figure 1) from the brances of *U. siamensis*. Their structures were determined through spectroscopic evidence (NMR and HRESIMS) and comparison with spectroscopic data from previous literature. Subsequently, compounds **1-8** were assessed for their antibacterial efficacy against both the *S. aureus* ATCC 25923 and MRSA strains, as well as for *α*-glucosidase inhibition and molecular docking study.

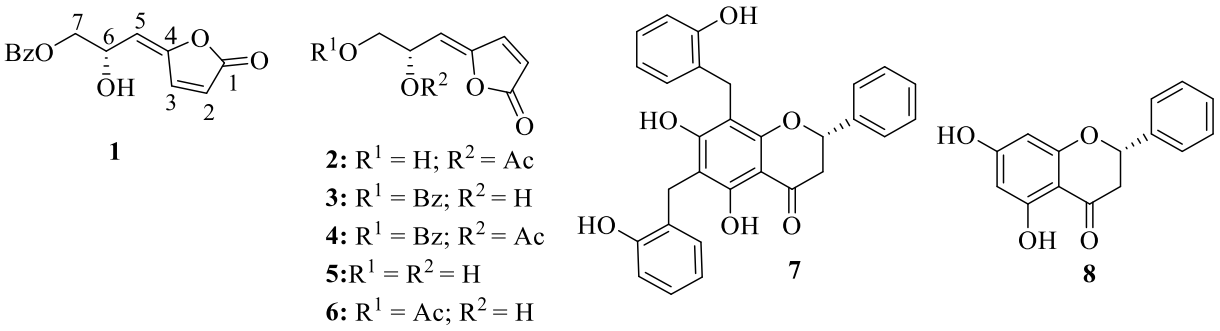

Figure 1. Chemical structures of **1-8**

2. Materials and Methods

2.1. General Experimental Procedures

A Bruker Avance III spectrometer operated at 500 MHz for ^{1}H NMR and 125 MHz for ^{13}C NMR, recorded 1D and 2D NMR spectra, with tetramethylsilane as an internal standard. HRESIMS was recorded using a MicrOTOF-Q mass spectrometer. Column chromatography was conducted on a silica gel (40-63 µm, Merck) column. For thin-layer chromatography (TLC), pre-coated silica gel 60 F_{254} or 60 RP-18 F_{254S} plates (Merck) were used. The TLC spots became visible after treatment with a 10% sulfuric acid solution and subsequent heating.

2.2. Plant Material

Branches of *U. siamensis* were collected in August 2023 from the Kaeng Khoi district, Saraburi province, Thailand. The plant material was identified by Dr. Suttitra Khumkratok (Walai Rukhavej Botanical Research Institute, Thailand) and Assoc. Prof. Dr. Dang Van Son (Institute of Tropical Biology, Vietnam). A voucher specimen (VNM-Huy05.24) was deposited at the herbarium of the Institute of Tropical Biology, Vietnam Academy of Science and Technology.

2.3. Extraction and Isolation

The dried branches of *U. siamensis* (15 kg) were ground and then subjected to maceration with EtOAc (30 L × 3, weekly) at room temperature. This process yielded EtOAc extract (132.25 g). This crude extract was subsequently loaded onto normal-phase silica gel column chromatography (CC) using a gradient system and eluted with a mixture of *n*-hexane and EtOAc (2:1-0:1, v/v). The procedure yielded 14 fractions (EA1-EA14), which subsequently were assessed for antimicrobial activity (Table S1). As a result, fractions EA8 and EA9 were selected for further analysis due to their strong activity. The purification process of these two fractions was illustrated in Scheme S1.
(*Z*)-6-Acetylsphaerodol (**2**). Colorless oil; $[\alpha]^{20}_{D}$ +125 (*c* 0.1, MeOH). ^{1}H NMR and ^{13}C NMR data (both in acetone-d_6): See Table 1. HRESIMS *m/z* 199.0638 (calcd. for $[C_9H_{10}O_5+H]^+$, 199.0606).

2.4. Antimicrobial Activity Assay

The antibacterial effects of the EtOAc extract, its fractions, and compounds **1-8** against both *S. aureus* ATCC 25923 and methicillin-resistant *S. aureus* (MRSA) strains were examined using the agar diffusion method. Solutions of the EtOAc extract and its fractions were prepared by dissolving in dimethyl sulfoxide (DMSO) at a concentration of 10 mg/mL, except for fractions EA10, EA12, and EA13, which were prepared at 2 mg/mL. Compounds **1-8** were diluted in DMSO at a concentration of 1 mg/mL. Bacterial strains were cultured overnight on nutrient agar at 37°C, and then diluted using sterile 0.9% NaCl to achieve bacterial suspensions with an OD_{600} of 0.1. Bacterial suspensions (100 μL) were spread on Mueller-Hinton agar (MHA) plates, and wells were created using sterile tips. Solutions of the EtOAc extract, its fractions, and isolated compounds in DMSO (50 μL each) were added to the created wells. The MHA plates were then placed in an incubator at 37°C for a period of 16-18 hours. Then, the inhibition zones of each well were measured. Positive and negative controls are apramycin (1 mg/mL) and DMSO, respectively.

2.5. Minimum Inhibitory Concentration

Compounds **4** and **6** were dissolved in DMSO and then further diluted in MeOH:HCl (MHA) to establish a range of concentrations from 0, 1, 2, 4, 8, 16, 32, 54, 128, and 256 μg/mL for each compound and these concentrations were put in wells of a 24-well plate. Then, 10^4 CFU of *S. aureus* ATCC 25923 and methicillin-resistant *S. aureus* (MRSA) were placed on the surface of the wells containing the concentration range of **4** and **6**. The plate was placed in an incubator at 37°C for 16-18 hours. The Minimum Inhibitory Concentration (MIC) values were found at the lowest concentration of as **4** and **6**, effectively inhibiting the growth of both *S. aureus* ATCC 25923 and methicillin-resistant *S. aureus* (MRSA) strains.

2.6. α-Glucosidase Inhibition Assay

The inhibitory activity of **1-8** against yeast α-glucosidase was evaluated according to a procedure previously described in the literature [20].

2.7. Molecular Docking Study

The protein receptor utilized in this study was the 3D structure of α-glucosidase MAL12, acquired from the AlphaFold2 database [24, 25]. The structures of potent compounds **3** and **7** were built using Gaussview 6.0 and then optimized using density functional theory (DFT) with the B3LYP/6-31G* basis set in Gaussian 16 [26]. To investigate the interactions between the inhibitors and α-glucosidase, molecular docking analyses were performed using AutoDock Vina 1.1.2. The docking input files were generated using the AutoDockTools 1.5.6 package. The highest-rated Vina docking score was selected and subsequently analyzed visually using PLIP [27] software and PyMOL.

3. Results and Discussion

The molecular formula of **2**, $C_9H_{10}O_5$, was established by HRESIMS through a protonated molecular ion peak at *m/z* 199.0638 $[M+H]^+$ (calcd. for $[C_9H_{10}O_5+H]^+$, 199.0606). ^{1}H NMR and HSQC spectra of **2** displayed two *cis*-coupled olefin protons (δ_H 7.75 and 6.37), a doublet olefinic proton (δ_H 5.46, d, J = 8.5 Hz) coupled with an oxymethine proton (δ_H 5.77, dt, J = 8.5, 5.5 Hz), and one diastereotopic methylene group (δ_H 3.73). The ^{13}C NMR data, consistent with HRESI mass data, exhibited nine carbon signals, including two ester carbons (δ_C 170.3 and 169.7), four olefinic carbons (δ_C 155.5, 145.4, 121.4, and 111.4), two oxygenated carbons (δ_C 71.2 and 64.0), and one methoxy group (δ_C 20.9) (Table 1). All the aforementioned spectroscopic data indicated that **2** was a γ-butenoid compound sharing a similar skeleton to **3-6**. HMBC networks of H-2 (δ_H 7.75) and H-3 (δ_H 6.37) to C-1 (δ_C 169.7) defined the γ-lactone ring. ^{1}H-^{1}H spin-spin interactions between H-2/H-3 and H-5/H-6/H-7 defined the connectivities through C-1 to C-7. The NMR data of **2** closely resembled those of **6** (Table 1), except for the presence of an acetyl group at C-6. This was indicated by a downfield chemical shift of H-6 (δ_H 5.75, dt, J = 8.0, 5.5 Hz). The double triplet status of this proton also confirmed the absence of 6-OH. Accordingly, the chemical structure of **2** was assigned as depicted in Figure 1.

The main constituents of *U. siamensis* were considered to be the γ-butenoids **1-7**. Many synthetic studies were conducted to validate their absolute configuration [11, 23]. Chakchaisiri *et al* determined that natural γ-butenoids in *U. siamensis* should have a 6*S* configuration, and their specific rotation at a particular concentration serves as evidence to distinguish the stereochemistry [11]. The distinction between the *E* configuration (in **1**) and the *Z* configuration (in **2-6**) was possible through NMR chemical shifts. In the same deuterated solvent, the H-3 proton of an *E* isomer displayed notably greater deshielding compared to that of a *Z* isomer. Furthermore, the carbon C-3 experienced an upfield shift of approximately 5 ppm [13]. NOESY network of H-3 and H-5 in **2** supported these previous findings (Figure 2). The positive optical rotation of **2-6** indicated a 6*S* configuration, while the negative optical rotation of **1** defined its 6*R* configuration. Compounds **7-8** were determined to have the 2*S* configuration based on their negative rotation.

Table 1. ^{1}H (500 MHz, δ_H, multi., J in Hz) and ^{13}C (125 MHz) NMR data of **2** and **6** in acetone-d_6.

Position	**2**		**6**	
	δ_H	δ_C	δ_H	δ_C
1		169.7		169.8
2	6.37 (1H, d, J = 5.5 Hz)	121.4	6.35 (1H, d, J = 5.5 Hz)	121.1
3	7.75 (1H, d, J = 5.5 Hz)	145.4	7.75 (1H, d, J = 5.5 Hz)	145.5
4		155.5		150.7
5	5.46 (1H, d, J = 8.5 Hz)	111.4	5.47 (1H, d, J = 9.0 Hz)	115.1
6	5.77 (1H, dt, J = 8.5, 5.5 Hz)	71.2	4.90 (1H, m)	65.3
7	3.73 (2H, t, 5.5 Hz)	64.0	4.08 (1H, dd, J = 11.0, 5.0 Hz) 4.15 (1H, dd, J = 11.0, 6.5 Hz)	67.5
6-OAc		170.3		
	2.03 (3H, s)	20.9		
7-OAc			2.00 (3H, s)	170.9 20.7

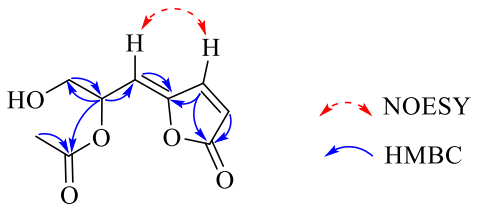

Figure 2. Selected HMBC and NOESY correlations of **2**

Fractions EA1-EA14 were assessed for their antimicrobial potential against two strains of *S. aureus*: ATCC 25923 and MRSA strains (Table S1). Fractions EA8 and EA9 were the most active fractions, which were then selected for further chemical analysis and consequently led to the isolation of **1-8**. Compounds **1-8** were tested for their activity on the aforementioned two *S. aureus* strains and revealed that **4** and **6** were the most active compounds, with inhibition zones of 12 and 13 mm against *S. aureus* ATCC 25923 and the MRSA strains, respectively. The MIC values of **4** and **6** were higher than 256 μg/mL, indicating their weak activity toward two tested *S. aureus* strains. This indicated that the presence of a free OH group at C-7 would decrease the activity, as observed in cases **2** and **5**. A comparison between **3** and **4** highlights the important role of 6-OAc in antimicrobial activity.

Compounds **1-8** were examined for their inhibition of α-glucosidase. Compounds **3** and **7** demonstrated significant efficacy, with IC_{50} values of 157 ± 15.0 and 94.2 ± 7.7 μM, respectively, when compared to the positive control acarbose (IC_{50} 331 ± 4.2 μM) (Table 2). The remaining compounds were inactive (IC_{50} >200 μM). For γ-butenoids **1-6**, the presence of the acetyl group at either C-6 or C-7 would decrease the activity. It is worth noting that there is limited existing research on the α-glucosidase inhibition of **1-8**.

Table 2. α-Glucosidase inhibitory activity of **1-8**.

Compound	IC_{50} (μM)
1	>200
2	>200
3	157 ± 15.0
4	>200
5	>200
6	>200
7	94.2 ± 7.7
8	>200
Acarbose	331 ± 4.2

Molecular docking serves as a valuable approach to elucidate the interaction mechanism between a ligand and a receptor, while also providing predictions for the potential binding sites of the ligand. Two active compounds **3** and **7** were docked into the active site of the *Saccharomyces cerevisiae* α-glucosidase, and the outcome was illustrated in Figure 3.

The evaluated binding energies between the α-glucosidase and **3** and **7** were −8.4 kcal.mol^{-1} and −9.4 kcal.mol^{-1}, respectively. As depicted in Figure 3, when bound to α-glucosidase, **3** formed a hydrogen bond with Gln181 and hydrophobic interactions with Tyr71, Phe157, Phe177, Thr215, Leu218, Glu276, Ala278, and Phe300. For compound **7**, its two hydroxyl groups formed hydrogen bonds with Arg-213 (2.02 Å) and Arg-439 (3.14 Å), and its phenyl group formed Pi-interactions with Tyr-71. Additionally, a hydrophobic patch comprising Phe157, Phe158, Phe177, Thr215, Leu218, Glu276, Ala278, and Phe300 enclosed and participated in hydrophobic interactions with **7**. The docking outcomes showed that **7** exhibited higher activity compared to **3** because it formed more hydrogen bonds and had lower binding energy. Previous studies have indicated that the formation of hydrogen bonds could play a role in increasing the stability of the complex [28]. As a result, the inhibitor attaches more firmly to the enzyme, leading to an increase in its inhibitory activity. The contribution of Pi-effects is crucial in protein-ligand recognition, as they contribute a substantial amount of binding enthalpy [29]. To summarize, the predominant interaction forces between our inhibitors and α-glucosidase may involve hydrogen bonding and hydrophobic interactions.

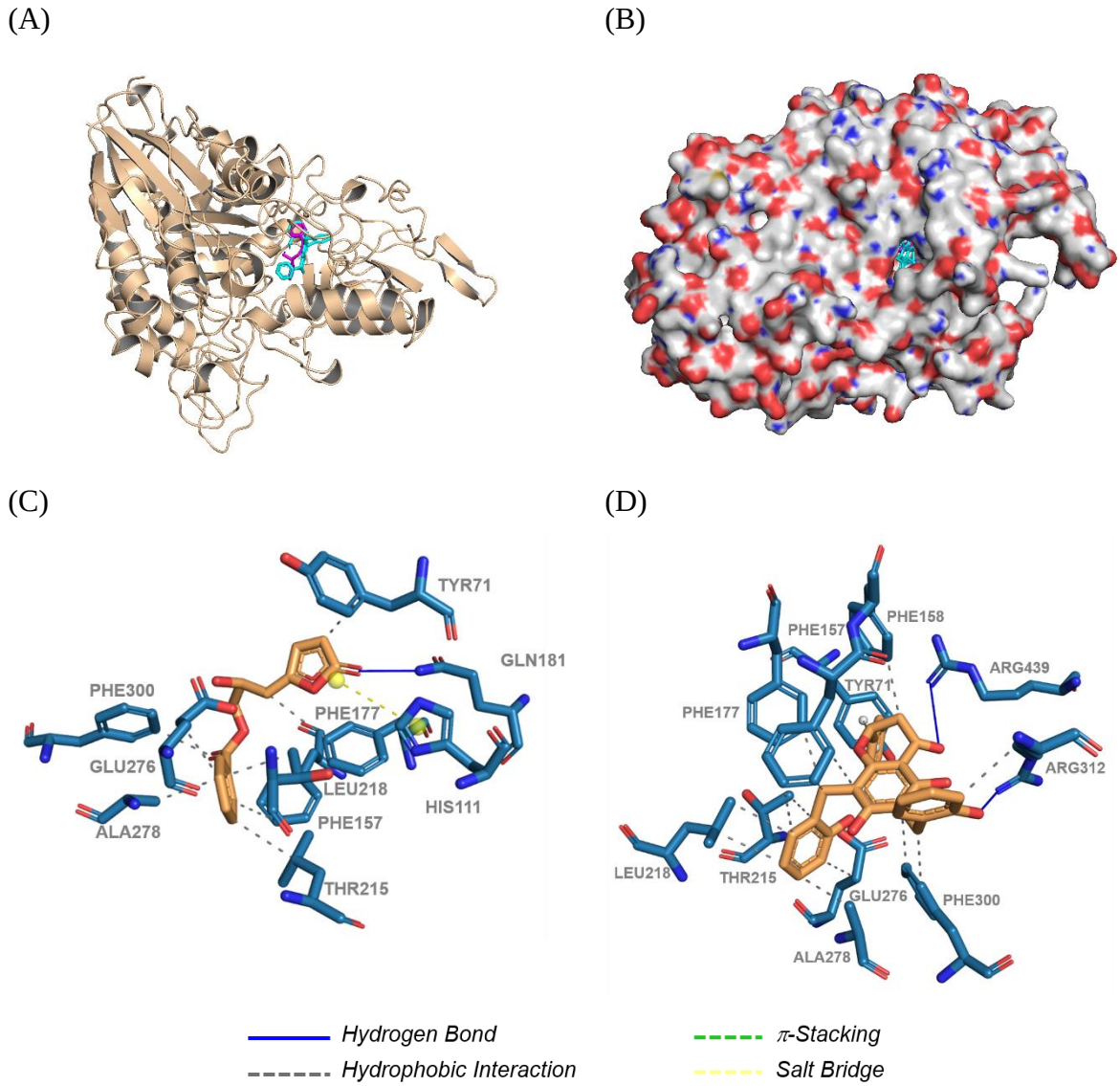

Figure 3. (A–B) Binding modes of **3** (magenta) and **7** (cyan) in *α*-glucosidase; **(C–E)** Detailed interactions of **3** and **7**

Acknowledgment

This study was supported by Thammasat University Research Unit in Natural Products Chemistry and Bioactivities (chemicals and biological tests).

Supporting Information

Supporting information accompanies this paper on http://www.acgpubs.org/journal/records-of-natural-products

ORCID
Ngoc-Hong Nguyen: 0000-0002-3119-1802
Boi-Phong Vuong: 0009-0006-8443-1079
Chuong Hoang Nguyen: 0000-0001-8317-7298
A Dong Huynh: 0009-0003-3316-7691

Dinh-Manh Nguyen: 0009-0008-2155-0139
Thuc-Huy Duong: 0000-0001-9891-4326
Hoang-Thanh Kpa: 0009-0003-8802-572X
Thi-Kim-Dung Le: 0000-0002-7847-5095
Thi-Ngoc-Duyen Nguyen: 0009-0009-0403-6426
Huy Truong Nguyen: 0000-0002-7725-9876
Jirapast Sichaem: 0000-0003-1407-496X

References

[1] T. D. Thang, D. N. Dai, T. M. Hoi and I. A. Ogunwande (2013). Essential oils from five species of Annonaceae from Vietnam, *Nat. Prod. Commun.* **8**, 239–242.

[2] I. M. Turner (2018). Annonaceae of the Asia-Pacific region: names, types and distributions, *Gard. Bull. Singapore* **70**, 409-744.

[3] D. M. Johnson, P. Bunchalee, P. Chalermglin, P. Chantaranothai, C. Leeratiwong, N.A. Murray, R. Saunders, Y. Sirichamorn, Y. Su and P. Sutthisaksopon (2021). Additions to annonaceae in the flora of Thailand, *Thai For. Bull. (Bot).* **49**, 163–172.

[4] G. Tanabe, Y. Manse, T. Ogawa, N. Sonoda, S. Marumoto, F. Ishikawa, K. Ninomiya, S. Chaipech, Y. Pongpiriyadacha, O. Muraoka and T. Morikawa (2018). Total synthesis of γ-alkylidenebutenolides, potent melanogenesis inhibitors from Thai medicinal plant *Melodorum fruticosum*, *J. Org. Chem.* **83**, 8250–8264.

[5] N. S. Engels, B. Waltenberger, S. Schwaiger, L. Huynh, H. Tran and H. Stuppner (2019). Melodamide A from *Melodorum fruticosum*-quantification using HPLC and one-step-isolation by centrifugal partition chromatography, *J. Sep. Sci.* **42**, 3165–3172.

[6] S. Hongnak, J. Jongaramruong, S. Khumkratok, P. Siriphong and S. Tip-pyang (2015). Chemical constituents and derivatization of melodorinol from the roots of *Melodorum fruticosum*, *Nat. Prod. Commun*. **10**, 633–636.

[7] H. H. Chan, T. L. Hwang, T. Thang, Y. L. Leu, P. C. Kuo, B. Nguyet, D. Dai and T. S. Wu (2013). Isolation and synthesis of melodamide A, a new anti-inflammatory phenolic amide from the leaves of *Melodorum fruticosum*, *Planta Med*. **79**, 288–294.

[8] R. Mongkol, J. Piapukiew and W. Chavasiri (2016). Chemical constituents from *Melodorum fruticosum* Lour. flowers against plant pathogenic fungi, *Agr. Nat. Resour.* **50**, 270–275.

[9] P. Pripdeevech (2011). Analysis of odor constituents of *Melodorum fruticosum* flowers by solid-phase microextraction-gas chromatography-mass spectrometry, *Chem. Nat. Compd.* **47**, 292–294.

[10] K. Sakulnarmrat and I. Konczak (2022). Encapsulation of *Melodorum fruticosum* Lour. anthocyanin-rich extract and its incorporation into model food, *LWT.* **153**, 112546.

[11] C. Chaichantipyuth, S. Tiyaworanan, S. Mekaroonreung, N. Ngamrojnavanich, S. Roengsumran, S. Puthong, A. Petsom and T. Ishikawa (2001). Oxidized heptenes from flowers of *Melodorum fruticosum*, *Phytochemistry* **58**, 1311–1315.

[12] A. Barco, S. Benetti, C. De Risi, G. P. Pollini, R. Romagnoli and V. Zanirato (1994). Synthesis of melodienone and 7-hydroxy-6-hydromelodienone, two heptenes from *Melodorum fruticosum*, *Tetrahedron* **50**, 10491–10496.

[13] P. Tuchinda, J. Udchachon, V. Reutrakul, T. Santisuk, W. C. Taylor, N. R. Farnsworth, J. M. Pezzuto and A. D. Kinghorn (1991). Bioactive butenolides from *Melodorum fruticosum*, *Phytochemistry* 3**0**, 2685–2689.

[14] L. T. M. Do and J. Sichaem (2022). New flavonoid derivatives from *Melodorum fruticosum* and their α-glucosidase inhibitory and cytotoxic activities, *Molecules* **27**, 4023–4031.

[15] J. H. Jung, S. Pummangura, C. Chaichantipyuth, C. Patarapanich, P. E. Fanwick, C. J. Chang and J. L. Mclaughlin (1990). New bioactive heptenes from *Melodorum fruticosum* (annonaceae), *Tetrahedron* **46**, 5043–5054.

[16] J. H. Jung, C. J. Chang, D. L. Smith, J. L. McLaughlin, S. Pummangura, C. Chaichantipyuth and C. Patarapanich (1991). Additional bioactive heptenes from *Melodorum fruticosum*, *J. Nat. Prod.* **54**, 500–505.

[17] P. Pripdeevech and E. Chukeatirote (2010). Chemical compositions, antifungal and antioxidant activities of essential oil and various extracts of *Melodorum fruticosum* L. flowers, *Food Chem. Toxicol.* **48**, 286-290.

[18] C. Kretzer, P. M. Jordan, K. P. L. Meyer, D. Hoff, M. Werner, R. K. Hofstetter, A. Koeberle, A. Cala Peralta, G. Viault, D. Seraphin, P. Richomme, J. J. Helesbeux, H. Stuppner, V. Temml, D. Schuster and O. Werz (2022). Natural chalcones elicit formation of specialized pro-resolving mediators and related 15-lipoxygenase products in human macrophages, *Biochem. Pharmacol.* **195**, 114825.

[19] A. W. Salae O. Chairerk, P. Sukkoet, T. Chairat, U. Prawat, P. Tuntiwachwuttikul, P. Chalermglin and S. Ruchirawat (2017). Antiplasmodial dimeric chalcone derivatives from the roots of *Uvaria siamensis*, *Phytochemistry* **135**, 135-143.

[20] H. T. M. Nguyen, D. T. T. Ngo, P. D. N, Nguyen, T. N. K, Pham, L. T. M. Do and J. Sichaem (2023). New prenyl flavanone and diarylbutanol from *Uvaria siamensis* stem bark and their α-glucosidase inhibitory activity, *Nat. Prod. Res.* 1-7, doi: 10.1080/14786419.2023.2272024.

[21] H. T. M. Nguyen, P. K. P. Nguyen, D. T. T. Ngo, J. Sichaem and L. T. M. Do (2022). Two new dimethylpyranoflavanones from the roots of *Melodorum fruticosum*, *Nat. Prod. Res.* **38** 433–439.

[22] G. Maeda, J. J. E. Munissi, S. Lindblad, S. Duffy, J. Pelletier, V. M. Avery, S. S. Nyandoro and M. Erdélyi (2020). A meroisoprenoid, heptenolides, and *C*-benzylated flavonoids from *Sphaerocoryne gracilis* ssp. *gracilis*, *J. Nat. Prod.* **83**, 316-322.

[23] T. Khotavivattana, T. Khamkhenshorngphanuch, K. Rassamee, P. Siripong and T. Vilaivan (2018). Diverted total synthesis of melodorinol analogues and evaluation of their cytotoxicity, *Tetrahedron Lett.* **59**, 2711–2715.

[24] J. Jumper, R. Evans, A. Pritzel, T. Green, M. Figurnov, O. Ronneberger, K. Tunyasuvunakool, R. Bates, A. Žídek, A. Potapenko (2021). Highly accurate protein structure prediction with AlphaFold, *Nature* **596**, 583-589.

[25] M. Varadi, S. Anyango, M. Deshpande, S. Nair, C. Natassia, G. Yordanova, D. Yuan, O. Stroe, G. Wood, A. Laydon, (2022). AlphaFold Protein Structure Database: massively expanding the structural coverage of protein-sequence space with high-accuracy models, *Nucleic Acid. Res.* **50**, D439-D444.

[26] M. J. Frisch, G. W. Trucks, H. B. Schlegel, G. E. Scuseria, M. A. Robb, J. R. Cheeseman, G. Scalmani, V. Barone, G. A. Petersson, H. Nakatsuji, X. Li, M. Caricato, A. V. Marenich, J. Bloino, B. G. Janesko, R. Gomperts, B. Mennucci, H.P. Hratchian, J.V. Ortiz, A.F. Izmaylov, J.L. Sonnenberg, Williams, F. Ding, F. Lipparini, F. Egidi, J. Goings, B. Peng, A. Petrone, T. Henderson, D. Ranasinghe, V. G. Zakrzewski, J. Gao, N. Rega, G. Zheng, W. Liang, M. Hada, M. Ehara, K. Toyota, R. Fukuda, J. Hasegawa, M. Ishida, T. Nakajima, Y. Honda, O. Kitao, H. Nakai, T. Vreven, K. Throssell, J. A. Montgomery Jr., J. E. Peralta, F. Ogliaro, M. J. Bearpark, J. J. Heyd, E. N. Brothers, K. N. Kudin, V. N. Staroverov, T. A. Keith, R. Kobayashi, J. Normand, K. Raghavachari, A. P. Rendell, J. C. Burant, S. S. Iyengar, J. Tomasi, M. Cossi, J. M. Millam, M. Klene, C. Adamo, R. Cammi, J. W. Ochterski, R. L. Martin, K. Morokuma, O. Farkas, J. B. Foresman, D. J. Fox (2016). Gaussian 16 Rev. C.01, Wallingford, CT.

[27] M. F. Adasme, K. L. Linnemann, S. N. Bolz, F. Kaiser, S. Salentin, V. J. Haupt, M. Schroeder (2021). PLIP 2021: Expanding the scope of the protein–ligand interaction profiler to DNA and RNA, *Nucleic Acid. Res.* **49**, W530-W534.

[28] J. B. Maguire, S. E. Boyken, D. Baker and B. Kuhlman (2018). Rapid sampling of hydrogen bond networks for computational protein design, *J. Chem. Theory Comput.* **14** 2751-2760.

[29] E. A. Meyer, R. K. Castellano and F. Diederich (2003). Interactions with aromatic rings in chemical and biological recognition, *Angew. Chem., Int. Ed. Engl.* **42**, 1210-1250.